

# **Liver extracellular matrix-based nanofiber scaffolds for the culture of primary hepatocytes and drug screening**

## **1. Introduction**

Hepatotoxic drug screening is majorly performed in animal models or in the *in vitro* systems using stem cell derived primary hepatocytes or hepatic cell lines. Mice models are closer to humans in the case of drug metabolism (due to the resemblance of the P450 gene homolog)<sup>1-3</sup>. Drug toxicity of acetaminophen (APAP) overdose is well characterized and studied in mice models, but with bottlenecks such as high metabolism rate of drugs varying within species and gender in mice<sup>4,5</sup>. Immortalized hepatic cell lines are also not apt for drug screening purposes because they lack the major genes involved in drug metabolism. HepaRG cell line, has a closer resemblance to primary hepatocytes and is most widely used in recent times<sup>6,7</sup>. Primary hepatocytes are the gold standard to determine drug toxicity *in vitro*, however, they are usually difficult to be maintained in their native state and they also dedifferentiate into mesenchymal cell type within a few days of culture<sup>8-10</sup>. Thus, there is a need to culture these cells for long term and determine hepatotoxicity of drugs without compromising their functionality. To facilitate long-term growth and cultures of primary hepatocytes *in vitro*, several strategies have been tested in the past years. The limitation of using spheroids for drug testing is that there is a diffusion limit within the spheroids. The cells in the core of the spheroid do not effectively metabolize the drug supplemented in the media and thus the final results might be misleading<sup>11</sup>.

Tissue engineering techniques such as electrospinning, freeze drying, particulate leaching and solvent casting have been used for many years in the past to fabricate scaffolds for cells including hepatocytes. Electrospinning is the most appropriate technique to fabricate nano-scaffolds because nanofibers produced as a result of electrospinning closely mimic the dense

collagen network of the tissue ECM<sup>12-14</sup>. Nanofiber scaffolds provide a high surface-to-volume ratio, with an ability to incorporate more cells in limited space<sup>15</sup>, the diameter of nanofiber scaffolds provides optimum spatial arrangement suitable for integrin binding of the cells<sup>16</sup>. Cells cultured on these nanofiber scaffolds serve as a promising mimic to that of the natural tissue microenvironment thereby it is highly suitable to use these fabricated scaffolds as drug screening platforms. Several other studies have reported that the use of decellularized liver matrix and/or matrix-derived proteins improve the overall viability and functions of the hepatic cell types<sup>17-22</sup>. With this background knowledge, we hypothesized that nanofiber scaffolds fabricated with liver extracellular matrix can prolong the lifespan and functional activity of primary hepatocytes *in vitro* thereby serving as a platform for drug screening.

We developed electrospun nanofiber scaffolds using a synthetic polymer polylactic acid (PLA) along with native undigested decellularized liver extracellular matrix (LEM) to effectively culture viable and metabolically active primary rodent hepatocytes and to accurately predict the lethal dose *in vivo* of two major hepatotoxic drugs.

### **Objective 1**

- Fabrication of fully bioactive and biocompatible novel electrospun liver matrix-based nanofiber scaffolds.
- Maintenance of mature hepatocyte morphology and functions throughout the culture period with minimal deterioration and with maximal drug metabolizing activity on fabricated liver-specific scaffolds.

### **Objective 2**

- Comprehensive characterization of primary hepatocytes on fabricated liver-based scaffolds in terms of gene and protein expression and specific functions.

- Screening of major hepatotoxic drugs, on the metabolically active primary hepatocytes cultured on liver-specific scaffolds and assessment of drug toxicity
- Accurate prediction of *in vivo* lethal dose toxicity in rodents from primary rodent hepatocytes cultured *ex vivo* on fabricated scaffolds

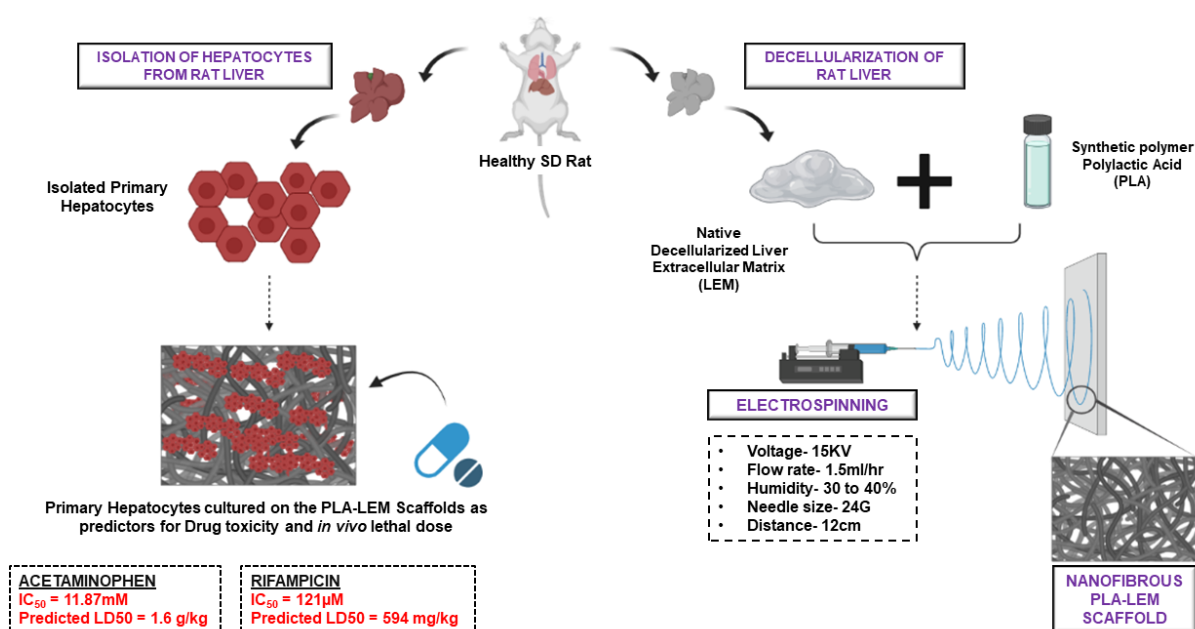


**Figure 1-** Graphical abstract of the study

## 2. Materials and Methods

### 2.1 Animal experiment and ethics

All Animals used in the experiments were housed and fed according to the guidelines of the Institutional Animal Ethics Committee (IAEC) at the Centre for Comparative Medicine, Institute of Liver and Biliary Sciences, Delhi. All the experimental protocols of isolating and culturing primary rodent hepatocytes and preparation of decell matrix were approved by IAEC protocol no. IAEC/ILBS/20/01.

## **2.2 Preparation of electrospinning solution and characterization of the electrospun scaffolds**

The electrospinning solution was prepared by mixing PLA and LEM in HFIP (Hexafluoroisopropanol) solvent. Nanofiber scaffolds were collected on aluminum foil and dried in a vacuum desiccator. The scaffolds were characterized by techniques such as SEM, FTIR, EDAX, Young's Modulus and contact angle estimation.

## **2.3 Drug toxicity assessment**

1 M stock solution of APAP and 25 mM stock solution of rifampicin was prepared by dissolving them in Dimethyl sulfoxide (DMSO). The working concentration of the drugs was further diluted with complete DMEM F12 (10%FBS, 1%Penstrep and 1% Antimycotic).

## **2.4 Lethal Dose (LD<sub>50</sub>) prediction of hepatotoxic drugs**

The half maximal inhibitory concentration (IC<sub>50</sub>) of the hepatotoxic drugs APAP and rifampicin was determined using MTT assay (3-(4,5-dimethylthiazol-2-yl)-2,5-diphenyl-2H-tetrazolium bromide). Drug treatment at varying concentrations was given to the primary hepatocytes on day 4 of culture on fabricated PLA-LEM scaffolds and RTC (Rat Tail Collagen) coated plates for 24 hrs., later the cells were washed with 1x PBS thrice. MTT assay was performed as mentioned earlier<sup>23,27</sup>. The LD<sub>50</sub> of the hepatotoxic drugs was determined with the formula,

$$\text{Log LD}_{50} = a + b * \text{Log (IC}_{50}) \quad (\text{Eqn 1})$$

The obtained LD<sub>50</sub> value was then divided by the density of the solution in which the drugs were dissolved to get a final LD<sub>50</sub> value (in terms of mg/kg).

## **3. Results**

### **3.1 Characterization of Decellularized liver extracellular matrix (LEM)**

LEM was prepared by perfusion of detergents through the portal vein of healthy SD rats. The appearance of the liver appeared white after each detergent treatment. The remnant detergents were removed by passing distilled water overnight. The acellularity of the liver post-decellularization was confirmed by Hematoxylin and Eosin staining (H&E Staining), DAPI staining and DNA estimation. A significant reduction of the DNA content in the decellularized liver in comparison to control liver was observed. The presence of LEM proteins post-decellularization was seen by histopathological staining namely Masson Trichrome staining, Alcian Blue and Orcein staining. Characterization of liver matrix post-decellularization has already been reported in our recent study<sup>24</sup>, which showed the presence of 149 LEM proteins. We also identified that 42% of the total ECM proteins contributed to the core matrisome and 58% contributed to the matrisome-associated protein category. After validating the complete removal of cells and the presence of intact matrix proteins, the LEM was used for the fabrication of the nanofiber scaffolds.

### **3.2 Physical characterization of fabricated PLA-LEM nanofiber scaffolds**

The LEM powder was mixed with the synthetic polymer solution, PLA to fabricate electrospun hybrid PLA-LEM scaffolds. The Scanning Electron Microscopy (SEM) analysis of the fabricated PLA-LEM hybrid scaffolds demonstrated uniform and homogeneous fiber distribution throughout the matrix. The formed fibers illustrated bead-free smooth texture with cylindrical morphology constituting a dense network with random orientation. With the incorporation of LEM, the fiber diameter of the electrospun PLA scaffolds increased when compared to polymer-only scaffolds. The pore size of the fabricated scaffolds also increased gradually with a concomitant increase in LEM incorporation PLA-LEM scaffolds depicted a pore size of  $38 \pm 8 \mu\text{m}$  ( $P=0.003$ ), which was in the range of an acellular liver tissue pore size<sup>25,26</sup>,

and also in the range of primary rat hepatocyte diameter<sup>27</sup>. To confirm the incorporation of LEM in the fabricated PLA-LEM mats we performed Energy dispersive X-ray spectroscopic (EDX) analysis. The addition of LEM in the PLA matrix introduced an additional nitrogen element, which was absent in the PLA group . The mean pore size distribution was further calculated using a capillary porometer that demonstrated a mean pore size of  $6.86 \pm 1.24 \mu\text{m}$  for PLA-LEM hybrid matrices when compared to the PLA group which had a mean pore size of  $2.81 \pm 0.79 \mu\text{m}$ . To determine the nature of the scaffold surfaces, we calculated the water contact angle. The PLA scaffolds depicted a contact angle of  $106.7 \pm 2.5^\circ$  whereas the PLA-LEM group showed a contact angle of  $61.55 \pm 1.42^\circ$ , suggesting decreased hydrophobicity in the PLA-LEM group . The *in vitro* swelling studies were then carried out for 10 days to decipher the water retention capability of the electrospun , the PLA-LEM sample group demonstrated an enhanced swelling ratio for all the time points than the PLA group. The mechanical property of the electrospun scaffolds assessed as a function of tensile modulus demonstrated a three-fold higher value for PLA scaffolds ( $1285.5 \pm 332.5 \text{ kPa}$ ) than PLA-LEM scaffolds ( $422.3 \pm 462.6 \text{ kPa}$ ).

### **3.3 Viability assessment of the cultured primary hepatocytes on PLA-LEM Scaffolds**

The viability of the hepatocytes cultured on the fabricated nanofiber scaffolds was estimated with Calcein and Sytox staining. We observed that the number of viable cells on the matrix containing hybrid scaffolds was higher than those cultured on RTC plates at all three-time points studied. On day 1, the number of live cells (green) and dead cells (red) on both the RTC as well as PLA-LEM scaffolds were almost similar. On day 10 we observed maximum viability of the hepatocytes cultured on the PLA-LEM group ( $83.8 \pm 3.0\%$ ) which was significantly higher than that of the RTC group at day 10 ( $47.5 \pm 3.0\%$ ,  $P < 0.001$ ).

### **3.4 Functional assessment of the cultured hepatocytes on PLALEM Scaffolds**

The albumin expression of primary hepatocytes cultured on PLA-LEM scaffolds was compared with those on PLA scaffolds and RTC as well. More albumin expressing cells were observed in the PLA-LEM group on both day 1 and day 4 of culture, although very few cells stained positive for albumin at day 10, yet they were higher than that of the RTC group. We observed a three-fold increase in the number of albumin-positive hepatocytes on the PLA-LEM scaffold ( $15 \pm 0.75\%$ ) when compared to the PLA group ( $4 \pm 0.5\%$ ,  $P=0.048$ ) and RTC group ( $5 \pm 0.5\%$ ;  $P=0.0002$ ) at day 4. Albumin secreted by the cultured primary hepatocytes on RTC, PLA and PLA-LEM scaffolds was also studied at day 1, 4 and 10 by rat albumin-specific ELISA. On day 4, we observed significantly higher production of albumin in the PLA-LEM group ( $\sim 450 \pm 26 \mu\text{g/ml}$ ;  $P=0.00004$ ) than that in the RTC group ( $\sim 310 \pm 34 \mu\text{g/ml}$ ). We further performed RT-PCR analysis of the hepatocytes seeded on the fabricated scaffolds. Cells on the PLA-LEM scaffolds showed increased expression of the hepatocyte-specific markers namely HNF4A (hepatocyte nuclear factor 4), ASGR1 (asialoglycoprotein receptor) and albumin up to 10 days in culture when compared to PLA and RTC groups. Overall, cells plated on PLA-LEM scaffolds demonstrated highest expression of the hepatic genes at day 4.

### **3.5 CYP Enzyme activity estimation**

After observing improved functions of the cultured primary hepatocytes on days 1 and 4 on the fabricated nanofiber scaffolds, we proceeded with these two-time points to assess the metabolic, i.e, Cytochrome P450 (CYP) enzyme activity of the hepatocytes in terms of Relative Light Units (RLU) at Day 1 and Day 4. Phenobarbital (Phenobarb), a well-known inducer of the CYP1A2 enzyme<sup>28</sup> was used here. On day 4, increased enzyme activity was seen only in the PLA-LEM group at all concentrations in comparison with the RTC and PLA groups. Maximum enzyme activity was seen with 1 mM concentration of Phenobarb on the PLA-LEM scaffold ( $3.5 \times 10^4$

$\pm 0.72 \times 10^3$  RLU). Overall, cells cultured on the PLA scaffolds showed minimal CYP activity on day 4 with all the concentrations of Phenobarb. .

### 3.6 Hepatotoxic Drug Screening with PLA-LEM Scaffolds

We investigated and compared the hepatotoxicity of two major drugs, APAP and Rifampicin on the fabricated scaffolds and RTC. Overall, highest toxicity was observed with the highest concentration of APAP (20 mM) and Rifampicin (150  $\mu$ M) in the PLA-LEM group. The  $IC_{50}$  of APAP was determined to be 11.87mM ( $R^2=0.98$ ) with the primary hepatocytes cultured on the PLA-LEM scaffolds, and with Eqn1, we were able to predict the lethal dose of APAP *in vivo* (1.6 g/kg). On the other hand, the  $IC_{50}$  of the primary hepatocytes cultured on the RTC plates was determined to be 3.2 mM ( $R^2=0.72$ ), with which the lethal dose through the Eqn 1 was determined to be 58 g/kg. The  $IC_{50}$  of Rifampicin was determined to be 121  $\mu$ M ( $R^2=0.97$ ) with primary hepatocytes cultured on the PLA-LEM scaffolds, with Eqn1 we were able to predict the lethal dose of APAP *in vivo* (574 mg/kg). On the other hand, the  $IC_{50}$  of primary hepatocytes cultured on RTC plates was determined to be 196  $\mu$ M ( $R^2=0.71$ ), with which the lethal dose predicted through the Eqn 1 came out to be around 23 mg/kg .

### 4. Statistical analysis

All data were analyzed using GraphPad Prism Software, version 6.01 (San Diego, CA, USA). Data are given as mean  $\pm$  standard deviation (SD). The difference between two groups was analyzed by the student 't' test.  $P < 0.05$  was considered significant.

### 5. Discussion

In the current study, we report the fabrication of a novel liver-specific nanofiber scaffold with pore size suitable for hepatocyte infiltration by the process of electrospinning for culturing primary hepatocytes. Our scaffolds served as a platform for maintenance of metabolically active



mature hepatocytes thereby facilitating optimal drug screening and hepatotoxicity prediction. Electrospun scaffolds containing pure ECM have not been widely explored by the scientific community, because pure ECM does not dissolve completely in organic solvents such as HFIP and chloroform which are widely used in electrospinning. Decellularized ECM has been mixed with wide variety of synthetic and natural polymers such as PCL, silk gelatin, alginate and chitosan in lesser concentrations to facilitate the formation of nanofibers<sup>29-31</sup>. In our study, we were not able to fabricate electrospun scaffolds with LEM alone due to the low viscosity of the solution. The hybrid scaffolds fabricated in our study however did not require any external cross-linking agent since we did not fragment the matrix proteins before mixing them with the polymer solution before electrospinning. Bual *et al*, utilized pepsin-digested porcine-derived LEM to culture primary hepatocytes for up to 7 days<sup>17</sup>. In our study, we used the crude decellularized LEM without pepsin digestion, so as to mimic the unfragmented matrix protein composition of the native tissue<sup>32,33</sup>. We standardized optimum electrospinning parameters for fabricating matrix-incorporated nanofiber scaffolds to culture primary hepatocytes. The pore size of the hybrid PLA-LEM electrospun scaffold was in the range (30-40 $\mu$ m)<sup>26,30,31</sup> suitable for hepatocyte infiltration thereby making it ideal for mimicking the native liver tissue microarchitecture under *in vitro* conditions. The HFIP solvent used for mixing LEM was completely evaporated during the electrospinning process and there was no residual solvent on the scaffolds that could prove cytotoxic. The decrease in hydrophobicity of the scaffold surface post-LEM incorporation made it suitable for the cells to adhere. Primary rat hepatocytes cultured on the PLA-LEM scaffolds showed better attachment, spreading and morphology when compared to the PLA scaffolds. Cell viability, albumin expression and secretion of the seeded hepatocytes were also higher on these hybrid scaffolds when compared to the PLA scaffolds and RTC even at day 10 of the cultures,

indicating that these scaffolds are superior in maintaining viable and functional hepatocytes. Morphology of the cultured hepatocytes was maintained on the PLA-LEM scaffolds until 10 days in culture unlike the conventional RTC plates where the hepatocytes transdifferentiated into fibroblast-like cells. Also, cells plated on the hybrid scaffolds showed superior metabolic activity (CYP1A2 Activity) than the ones on the RTC-coated plates. Primary hepatocytes on LEM hybrid nanofiber scaffolds further demonstrated increased cytotoxicity at increasing concentrations of APAP and rifampicin similar to the study performed by Yokoyama *et al*,<sup>7</sup> where they have shown increased toxicity of HepaRG, HepG2 and cryopreserved primary human hepatocytes at increasing concentrations of various hepatotoxic drugs in scaffold-free *in vitro* cultures. We were able to effectively predict lethal dose of APAP (1.6g/kg) and rifampicin (594mg/kg) determined from the IC<sub>50</sub> values<sup>35-37</sup> of hepatocytes cultured on PLA-LEM scaffolds, which were in the range of those reported in the rodents (840 mg/kg - 2 g/kg and 100 mg/kg –600 mg/kg respectively)<sup>38-40</sup>. The LD<sub>50</sub> of the two drugs predicted from the IC<sub>50</sub> of hepatocytes on RTC did not fall in the reported range of toxicity *in vivo* since there was no linear regression in cytotoxicity values with respect to increasing drug concentration. We repeated this experiment several times to nullify any technical errors. Our study thus demonstrates the utility of hybrid PLA-LEM scaffolds in determining the *in vivo* lethal toxic dose of drugs thus acting as an accurate preclinical drug testing platform. We believe that primary hepatocytes cultured on our hybrid scaffolds would provide more homogenous results in terms of drug screening as compared to the 3D culture models as hepatocytes cultured in 3D in the form of spheroids and organoids do not proliferate effectively without subsequent passages<sup>41-43</sup>, thus leading to inconsistent results during drug screening experiments.

## **6. Impact of the research on the benefit of mankind**

- The nanofiber scaffolds with the primary rodent hepatocytes developed from this project can be used as an ex vivo hepatotoxic drug screening platform and transplantable cell sheets in vivo in liver injury. LEM fabricated in the form of hydrogels can also be used for in vivo cell transplantation to facilitate regeneration and repair in liver injury.
- The LEM-based scaffolds and hydrogels provide an optimum environment to support functionally and metabolically active primary rodent hepatocytes. These scaffolds along with the primary cells serve as a mimic to the native liver and thus can be utilized as a tool for hepatotoxic drug screening. From the cultured hepatocytes, we can also predict the lethal doses in vivo of unidentified/possible drugs that can cause hepatotoxicity in rodents. The same scaffolds can be modified with primary human hepatocytes to determine the lethal drug dosage in humans. The same scaffolds with primary hepatocytes may be used as transplant sheets to improve the regenerative capacity of the liver during injury. The LEM-based injectable hydrogels fabricated as a part of this project can also be used for in vivo transplantation with and without liver cells to facilitate regeneration and repair in liver injury.
- The developed electrospun LEM based nanofiber scaffolds may serve as a cost-effective solution for culturing of hepatocytes in 2D and 3D cultures to surpass the use of commercial matrix proteins such as collagen and fibronectin which are used as conventional coating for the culture of primary hepatocytes in vitro.

## References

1. McGill MR, Williams CD, Xie Y, Ramachandran A, Jaeschke H. APAP-induced liver injury in rats and mice: comparison of protein adducts, mitochondrial dysfunction, and oxidative stress in the mechanism of toxicity. *Toxicol Appl Pharmacol* **2012**;264:387-394. DOI: [10.1016/j.taap.2012.08.015](https://doi.org/10.1016/j.taap.2012.08.015)
2. Jaeschke H, Williams CD, McGill MR, Xie Y, Ramachandran A. Models of drug-induced liver injury for evaluation of phytotherapeutics and other natural products. *Food Chem Toxicol* **2013**;55:279-289 DOI: [10.1016/j.fct.2012.12.063](https://doi.org/10.1016/j.fct.2012.12.063)
3. McGill MR, Sharpe MR, Williams CD, Taha M, Curry SC, Jaeschke H. The mechanism underlying APAP-induced hepatotoxicity in humans and mice involves mitochondrial damage and nuclear DNA fragmentation. *J Clin Invest* **2012**;122:1574-1583. DOI: [10.1172/JCI59755](https://doi.org/10.1172/JCI59755)
4. Jaeschke H, Xie Y, McGill MR. APAP-induced liver injury: from animal models to humans. *Journal of clinical and translational hepatology*. **2014** Sep;2(3):153. DOI: [10.14218/JCTH.2014.00014](https://doi.org/10.14218/JCTH.2014.00014)
5. Xu Z, Kang Q, Yu Z, Tian L, Zhang J, Wang T. Research on the Species Difference of the Hepatotoxicity of Medicine Based on Transcriptome. *Frontiers in Pharmacology*. **2021** Apr 23;12:647084. DOI: [10.3389/fphar.2021.647084](https://doi.org/10.3389/fphar.2021.647084)
6. McGill MR, Yan HM, Ramachandran A, Murray GJ, Rollins DE, Jaeschke H. HepaRG cells: a human model to study mechanisms of APAP hepatotoxicity. *Hepatology*. **2011** Mar;53(3):974-82. DOI: [10.1002/hep.24132](https://doi.org/10.1002/hep.24132)

7. Yokoyama Y, Sasaki Y, Terasaki N, Kawataki T, Takekawa K, Iwase Y, Shimizu T, Sanoh S, Ohta S. Comparison of drug metabolism and its related hepatotoxic effects in HepaRG, cryopreserved human hepatocytes, and HepG2 cell cultures. *Biological and pharmaceutical bulletin*. **2018**;b17-00913. DOI: [10.1248/bpb.b17-00913](https://doi.org/10.1248/bpb.b17-00913)
8. Andersson, T.B.; Ingelman-Sundberg, M.; Heins, N. Hepatocyte-like cells derived from human embryonic stem cells specifically via definitive endoderm and a progenitor stage. *J. Biotechnol.* **2010**, *145*, 284–294. DOI: [10.1016/j.jbiotec.2009.11.007](https://doi.org/10.1016/j.jbiotec.2009.11.007)
9. Duan, Y.Y.; Catana, A.; Meng, Y.; Yamamoto, N.; He, S.Q.; Gupta, S.; Gambhir, S.S.; Zerna, M.A. Differentiation and enrichment of hepatocyte-like cells from human embryonic stem cells in vitro and in vivo. *Stem Cells* **2007**, *25*, 3058–3068. DOI: [10.1634/stemcells.2007-0291](https://doi.org/10.1634/stemcells.2007-0291)
10. Lavon, N.; Yanuka, O.; Benvenisty, N. Differentiation and isolation of hepatic-like cells from human embryonic stem cells. *Differentiation* **2004**, *72*, 230–238. DOI: [10.1111/j.1432-0436.2004.07205002.x](https://doi.org/10.1111/j.1432-0436.2004.07205002.x)
11. Wei J, Lu J, Chen M, Xie S, Wang T, Li X. 3D spheroids generated on carbon nanotube-functionalized fibrous scaffolds for drug metabolism and toxicity screening. *Biomaterials science*. **2020**;8(1):426-37. DOI: [10.1039/c9bm01310e](https://doi.org/10.1039/c9bm01310e)
12. Badylak SF, Freytes DO, Gilbert TW. Extracellular matrix as a biological scaffold material: Structure and function. *Acta biomaterialia*. **2009** Jan 1;5(1):1-3. DOI: [10.1016/j.actbio.2008.09.013](https://doi.org/10.1016/j.actbio.2008.09.013)

13. Vasudevan A, Tripathi DM, Sundarrajan S, Venugopal JR, Ramakrishna S, Kaur S. Evolution of Electrospinning in Liver Tissue Engineering. *Biomimetics*. **2022** Sep 30;7(4):149. DOI: [10.3390/biomimetics7040149](https://doi.org/10.3390/biomimetics7040149)
14. Ding, Y., Xu, W., Xu, T., Zhu, Z., & Fong, H. Theories and principles behind electrospinning. *Advanced Nanofibrous Materials Manufacture Technology Based on Electrospinning*. CRC Press, **2019** (pp. 22-51)
15. Park J, Bauer S, von der Mark K, Schmuki P. Nanosize and vitality: TiO<sub>2</sub> nanotube diameter directs cell fate. *Nano letters*. **2007** Jun 13;7(6):1686-91. DOI: [10.1021/nl070678d](https://doi.org/10.1021/nl070678d)
16. Cavalcanti-Adam EA, Aydin D, Hirschfeld-Warneken VC, Spatz JP. Cell adhesion and response to synthetic nanopatterned environments by steering receptor clustering and spatial location. *HFSP journal*. **2008** Oct 1;2(5):276-85. DOI: [10.2976/1.2976662](https://doi.org/10.2976/1.2976662)
17. Bual R, Kimura H, Ikegami Y, Shirakigawa N, Ijima H. Fabrication of liver-derived extracellular matrix nanofibers and functional evaluation in in vitro culture using primary hepatocytes. *Materialia*. **2018** Dec 1;4:518-28. doi.org/10.1016/j.mtla.2018.11.014
18. Grant R, Hallett J, Forbes S, Hay D, Callanan A. Blended electrospinning with human liver extracellular matrix for engineering new hepatic microenvironments. *Scientific reports*. **2019** Apr 18;9(1):1-2. DOI: [10.1038/s41598-019-42627-7](https://doi.org/10.1038/s41598-019-42627-7)
19. Grant R, Hay D, Callanan A. From scaffold to structure: the synthetic production of cell derived extracellular matrix for liver tissue engineering. *Biomedical Physics & Engineering Express*. **2018** Oct 17;4(6):065015. DOI 10.1088/2057-1976/aacbe1

20. Saheli M, Sepantafar M, Pournasr B, Farzaneh Z, Vosough M, Piryaee A, Baharvand H. Three-dimensional liver-derived extracellular matrix hydrogel promotes liver organoids function. *Journal of cellular biochemistry*. **2018** Jun;119(6):4320-33. DOI: [10.1002/jcb.26622](https://doi.org/10.1002/jcb.26622)
21. Hussein KH, Park KM, Yu L, Kwak HH, Woo HM. Decellularized hepatic extracellular matrix hydrogel attenuates hepatic stellate cell activation and liver fibrosis. *Materials Science and Engineering: C*. **2020** Nov 1;116:111160. DOI: [10.1016/j.msec.2020.111160](https://doi.org/10.1016/j.msec.2020.111160)
22. Ijima H, Nakamura S, Bual RP, Yoshida K. Liver-specific extracellular matrix hydrogel promotes liver-specific functions of hepatocytes in vitro and survival of transplanted hepatocytes in vivo. *Journal of bioscience and bioengineering*. **2019** Sep 1;128(3):365-72. DOI: [10.1016/j.jbiosc.2019.02.014](https://doi.org/10.1016/j.jbiosc.2019.02.014)
23. Sharma A, Rawal P, Tripathi DM, Alodiya D, Sarin SK, Kaur S, Ghosh S. Upgrading hepatic differentiation and functions on 3D printed silk–decellularized liver hybrid scaffolds. *Acs Biomaterials Science & Engineering*. **2021** Jul 28;7(8):3861-73. DOI: [10.1021/acsbiomaterials.1c00671](https://doi.org/10.1021/acsbiomaterials.1c00671)
24. Biswas, S., Vasudevan, A., Yadav, N., Yadav, S., Rawal, P., Kaur, I., Chauhan, V. S. Chemically modified dipeptide based hydrogel supports three-dimensional growth and functions of primary hepatocytes. *ACS Applied Bio Materials*, **2022**. 5(9), 4354-4365. <https://doi.org/10.1021/acsabm.2c00526>
25. Uygun BE, Soto-Gutierrez A, Yagi H, Izamis ML, Guzzardi MA, Shulman C, Milwid J, Kobayashi N, Tilles A, Berthiaume F, Hertl M, Nahmias Y, Yarmush ML, Uygun K. Organ reengineering through development of a transplantable recellularized liver graft

using decellularized liver matrix. *Nat Med.* **2010** Jul;16(7):814-20. doi: 10.1038/nm.2170.

26. Bate TS, Shanahan W, Casillo JP, Grant R, Forbes SJ, Callanan A. Rat liver ECM incorporated into electrospun polycaprolactone scaffolds as a platform for hepatocyte culture. *Journal of Biomedical Materials Research Part B: Applied Biomaterials.* **2022** Dec;110(12):2612-23. DOI: [10.1002/jbm.b.35115](https://doi.org/10.1002/jbm.b.35115)
27. Chakraborty J, Majumder N, Sharma A, Prasad S, Ghosh S. 3D bioprinted silk-reinforced Alginate-Gellan Gum constructs for cartilage regeneration. *Bioprinting.* **2022** Dec 1;28:e00232. 10.1016/j.bprint.2022.e00232
28. Sakuma T, Ohtake M, Katsurayama Y, Jarukamjorn K, Nemoto N. Induction of CYP1A2 by phenobarbital in the livers of aryl hydrocarbon-responsive and-nonresponsive mice. *Drug metabolism and disposition.* **1999** Mar 1;27(3):379-84.
29. Bishi DK, Mathapati S, Venugopal JR, Guhathakurta S, Cherian KM, Verma RS, Ramakrishna S. A Patient-Inspired Ex Vivo Liver Tissue Engineering Approach with Autologous Mesenchymal Stem Cells and Hepatogenic Serum. *Advanced healthcare materials.* **2016** May;5(9):1058-70. <https://doi.org/10.1002/adhm.201500897>
30. Kazemnejad S, Allameh A, Soleimani M, Gharehbaghian A, Mohammadi Y, Amirizadeh N, Esmacili S. Functional hepatocyte-like cells derived from human bone marrow mesenchymal stem cells on a novel 3-dimensional biocompatible nanofibrous scaffold. *The International Journal of Artificial Organs.* **2008** Jun;31(6):500-7. <https://doi.org/10.1177/039139880803100605>



31. Bishi DK, Mathapati S, Venugopal JR, Guhathakurta S, Cherian KM, Ramakrishna S, Verma RS. Trans-differentiation of human mesenchymal stem cells generates functional hepatospheres on poly (l-lactic acid)-co-poly ( $\epsilon$ -caprolactone)/collagen nanofibrous scaffolds. *Journal of Materials Chemistry B*. **2013**;1(32):3972-84. <https://doi.org/10.1039/C3TB20241K>
32. Brown B, Lindberg K, Reing J, Stolz DB, Badylak SF. The basement membrane component of biologic scaffolds derived from extracellular matrix. *Tissue engineering*. **2006** Mar 1;12(3):519-26. DOI: [10.1089/ten.2006.12.519](https://doi.org/10.1089/ten.2006.12.519)
33. Shoulders MD, Raines RT. Collagen structure and stability. *Annual review of biochemistry*. **2009**;78:929. DOI: [10.1146/annurev.biochem.77.032207.120833](https://doi.org/10.1146/annurev.biochem.77.032207.120833)
34. Martinez-Hernandez A, Amenta PS. The hepatic extracellular matrix. *Virchows Archiv A*. **1993** Mar;423(2):77-84. DOI: [10.1007/BF01606425](https://doi.org/10.1007/BF01606425)
35. Spielmann H, Genschow E, Liebsch M, Halle W. Determination of the starting dose for acute oral toxicity (LD50) testing in the up and down procedure (UDP) from cytotoxicity data. *Alternatives to Laboratory Animals*. **1999** Nov;27(6):957-66. DOI: [10.1177/026119299902700609](https://doi.org/10.1177/026119299902700609)
36. Garle MJ, Fentem JH, Fry JR. In vitro cytotoxicity tests for the prediction of acute toxicity in vivo. *Toxicology in vitro*. **1994** Dec 1;8(6):1303-12. DOI: [10.1016/0887-2333\(94\)90123-6](https://doi.org/10.1016/0887-2333(94)90123-6)
37. Halle W, Halder M, Worth A, Genschow E. The registry of cytotoxicity: toxicity testing in cell cultures to predict acute toxicity (LD50) and to reduce testing in animals.

Alternatives to Laboratory Animals. **2003** Mar;31(2):89.  
DOI: [10.1177/026119290303100204](https://doi.org/10.1177/026119290303100204)

38. Green MD, Shires TK, Fischer LJ. Hepatotoxicity of APAP in neonatal and young rats: I. Age-related changes in susceptibility. *Toxicology and applied pharmacology*. **1984** Jun 15;74(1):116-24. DOI: [10.1016/0041-008x\(84\)90277-1](https://doi.org/10.1016/0041-008x(84)90277-1)
39. McGill MR, Williams CD, Xie Y, Ramachandran A, Jaeschke H. APAP-induced liver injury in rats and mice: comparison of protein adducts, mitochondrial dysfunction, and oxidative stress in the mechanism of toxicity. *Toxicology and applied pharmacology*. **2012** Nov 1;264(3):387-94. DOI: [10.1016/j.taap.2012.08.015](https://doi.org/10.1016/j.taap.2012.08.015)
40. Kim JH, Nam WS, Kim SJ, Kwon OK, Seung EJ, Jo JJ, Shresha R, Lee TH, Jeon TW, Ki SH, Lee HS. Mechanism investigation of rifampicin-induced liver injury using comparative toxicoproteomics in mice. *International journal of molecular sciences*. **2017** Jul 2;18(7):1417. DOI: [10.3390/ijms18071417](https://doi.org/10.3390/ijms18071417)
41. Souza, A. G., Silva, I. B. B., Campos-Fernandez, E., Barcelos, L. S., Souza, J. B., Marangoni, K., Alonso-Goulart, V. Comparative assay of 2D and 3D cell culture models: proliferation, gene expression and anticancer drug response. *Current pharmaceutical design*, 24(15), **2018**. 1689-1694. <https://doi.org/10.2174/1381612824666180404152304>
42. Luca, A. C., Mersch, S., Deenen, R., Schmidt, S., Messner, I., Schäfer, K. L., Stoecklein, N. H. Impact of the 3D microenvironment on phenotype, gene expression, and EGFR inhibition of colorectal cancer cell lines. *PloS one*, 8(3), **2013**. e59689. <https://doi.org/10.1371/journal.pone.0059689>

43. Adcock, A. F., Trivedi, G., Edmondson, R., Spearman, C., Yang, L. Three-dimensional (3D) cell cultures in cell-based assays for in-vitro evaluation of anticancer drugs. *Journal of Analytical & Bioanalytical Techniques*, 6(3), **2015**. 1.  
<https://doi.org/10.3389/fphar.2018.00006>